Isolation and Characterization of Novel Oligosaccharides Related to Ziracin

Min Chu,* Ronald Mierzwa, John Jenkins, Tze-Ming Chan, Pradip Das, Birendra Pramanik, Mahesh Patel, and Vincent Gullo

Schering-Plough Research Institute, 2015 Galloping Hill Road, Kenilworth, New Jersey 07033

Received March 8, 2002

Five novel oligosaccharide antibiotics, Sch 58769 (**1**), Sch 58771 (**2**), Sch 58773 (**3**), Sch 58775 (**4**), and Sch 58777 (**5**), were isolated from the fermentation broth of *Micromonospora carbonacea* var *africana*. Their structures were determined by spectroscopic methods, including MS and ^{1}H and ^{13}C NMR experiments. A comparison of the obtained data with that for Ziracin (Sch 27899) revealed that these oligosaccharides belong to the same everninomicin family of compounds. Ziracin demonstrates potent activity against Gram-positive bacteria both in vitro and in vivo including multiply resistant strains of methicillin-resistant *Staphylococcus aureus* and vancomycin-resistant *Enterococci faecalis*.

The large number of potent broad-spectrum antibiotics introduced into clinical use over the past half-century has brought significant control over infectious diseases. However, the intensive use of antibiotics has also been accompanied by the rapid development of multiple antibiotic-resistant pathogenic bacteria during the past decade.[1,2] Recently, bacterial strains resistant to all available antibacterial agents have been identified among clinical isolates of some bacterial species.[3,4] Therefore, the discovery of new classes of antibiotics with novel mechanisms of action has now become a major challenge for the pharmaceutical industry. Everninomicins, a novel class of oligosaccharide antibiotics produced by *Micromonospora carbonaceae*, possess potent activity against Gram-positive bacteria, including vancomycin-resistant enterococci, methicillin-resistant staphylococci, and penicillin-resistant streptococci.[5] The fermentation product, Ziracin (Sch 27899), demonstrates the most potent activity against these strains.[6] In recent studies of the mechanism of action, Ziracin was reported to be a protein synthesis inhibitor with unique binding to ribosomal protein L16.[7] This novel mechanism of action for Ziracin provides a rationale for the susceptibility of multidrug-resistant bacterial pathogens to the everninomicin family of compounds. In the course of a large-scale purification of Ziracin, numerous minor components closely related to Ziracin were detected in the front and tail cuts from initial silica gel column chromatography. However, the separation of these minor components was not possible using conventional silica gel column chromatography, and therefore, a two-step chromatographic procedure using diol-bonded silica gel for enrichment followed by poly(vinyl alcohol)-functionalized silica gel (PVA-Sil) for purification was implemented.[8] As a result of this tandem normal-phase purification approach, five novel compounds were isolated and identified, namely, Sch 58769 (**1**), Sch 58771 (**2**), Sch 58773 (**3**), Sch 58775 (**4**), and Sch 58777 (**5**) as shown in Figures 1 and 2. This paper describes the isolation, purification, and structure elucidation of these oligosaccharides.

Results and Discussion

The source microorganism was isolated from a sample of mud obtained from the bank of the Nyiro River in Kenya, Africa. The strain was designated as *Micromonospora carbonacea* var *africana*.[9] A culture of this microorganism was sent to American Type Culture Collection (ATCC) in Rockville, MD, where it was assigned accession number ATCC 39149. The culture rarely forms spores. When the spores are present, they usually occur singly, are usually sessile, and appear along the length of 0.5−0.8 μm slightly branched vegetative mycelia. Well growth of the culture is found from 27 to 35 °C on yeast-dextrose agar with the formation of orange vegetative mycelial pigments and red to orange diffusable pigments.

As shown in Scheme 1, tail cut (5 g) from initial large-scale silica gel separation was dissolved in 20 mL of CH_2Cl_2/MeOH (96:4 v/v) and applied to 200 g (~400 mL) of preconditioned diol-bonded silica gel (40−63 μm, irregular media) contained in a glass column (600 × 50 mm, 1.18 L). The diol column was conditioned prior to sample application by washing with 1 L of MeOH followed by 1.2 L of initial mobile phase CH_2Cl_2/heptane/MeOH (60:40:2 v/v/v). After sample application, 2.4 L of mobile phase was collected, and then the ratio of mobile phase was adjusted to 75:25:2 (v/v) and maintained for an additional 8 L. Individual fractions (400 mL/fraction) were evaluated for the presence of targeted components by analytical HPLC. On the basis of analytical HPLC, fractions containing components **1** and **2** were pooled as complex 1. Complex 1 (100 mg) was further purified by dissolving 33 mg of the sample in 0.5 mL of CH_2Cl_2/MeOH (96:4 v/v) and injecting on a semipreparative PVA-Sil column (250 × 20 mm), equilibrated with CH_2Cl_2/heptane/MeOH (78:20:2 v/v/v) solvent system at a flow rate of 12 mL/min under UV detection of 265 nm. After two additional injections were made for the remaining material (33 mg of each injection on the HPLC column using the same conditions as described above), two pure compounds, **1** (1.5 mg) and **2** (9.5 mg), were obtained from 100 mg of complex 1.

The sample of front cut (5 g) was dissolved in 25 mL of CH_2Cl_2/MeOH (96:4 v/v) and applied to 200 g of a recycled diol-bonded silica column. Recycling involved passing 1.5 L of MeOH followed by 1.5 L of starting mobile phase CH_2Cl_2/heptane/MeOH (60:40:2 v/v/v). After sample application, 2.8 L of mobile phase was collected and the effluent discarded. The mobile phase was adjusted to 75:25:2 (v/v/v), and 400 mL fractions were collected. Fractions containing components **3**, **4**, and **5** were pooled as complex 2, yielding 61 mg of white powder after rotary evaporation. Optimization studies for preparative chromatography led to the selection of a binary solvent system composed of

* To whom correspondence should be addressed. Tel: (908) 740-7290. Fax: (908) 740-7115. E-mail: min.chu@spcorp.com.

10.1021/np020093t CCC: $22.00
Published on Web 09/13/2002

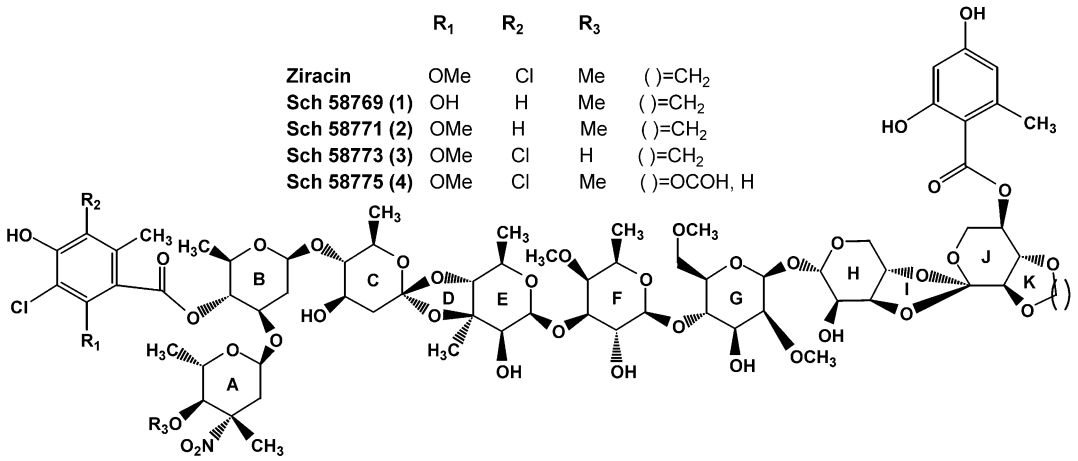

Figure 1. Structures of Ziracin and analogues **1**−**4**.

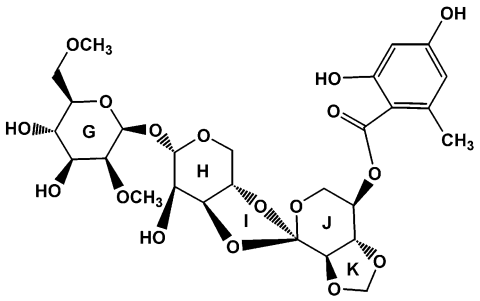

Figure 2. Structure of Sch 58777 (**5**).

Scheme 1. Isolation of Compounds **1**−**5**

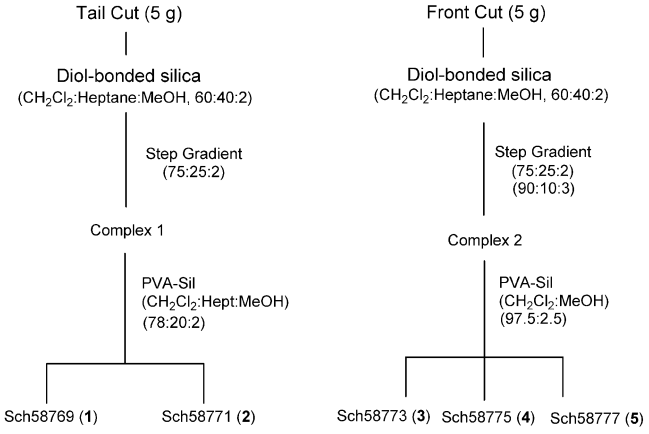

n-butyl chloride (n-BuCl)/MeOH. Approximately 30 mg of complex 2 was then dissolved in 1.0 mL of CH_2Cl_2/MeOH (96:4 v/v) and injected on a semipreparative PVA-Sil column (250 × 20 mm), equilibrated with n-BuCl/MeOH (93:7 v/v) at flow rate of 15 mL/min under UV detection of 265 nm. Three pure components, **3** (6.1 mg), **4** (8.7 mg), and **5** (27.5 mg), were obtained after two PVA-Sil HPLC runs.

All compounds were obtained as white powders after removal of solvents. The compounds were soluble in MeOH, DMSO, EtOAc, acetone, and $CHCl_3$; partially soluble in Et_2O, CH_2Cl_2, and n-BuCl; insoluble in hexane, petroleum ether, and H_2O. The physicochemical properties and spectroscopic data of **1**−**5** are summarized in Table 1.

Structure determination of compounds **1**−**5** was accomplished by spectroscopic data analyses, including fast atom bombardment mass spectrometry (FABMS) and ^1H and ^{13}C NMR spectral data. In previous studies, since the detailed structural assignments of Ziracin were well documented on the basis of extensive spectroscopic data analysis, the FABMS and NMR data of Ziracin served as a reference and allowed direct comparison to elucidate the structures of the analogues **1**−**5**.[10]

Compound **1** showed a molecular weight of 1581 based on FABMS data that revealed a protonated molecular ion at *m/z* 1582 $(M + H)^+$. The negative FABMS data of **1** confirmed the positive mode data by showing a deprotonated ion peak at *m/z* 1580 $(M - H)^-$. The isotope cluster pattern of **1** suggested the presence of one chlorine atom. The molecular weight of 1581 for **1** indicated 48 mass units less than Ziracin (see Figure 3). Further examination of individual fragments of **1** as shown in Figure 4 revealed that the right side portion was identical to Ziracin. The left side aromatic residue showed a 48 mass unit decrease by sequential breakdown fragment analysis at *m/z* 502 and 185 in comparison with Ziracin. The ^1H NMR spectral data of **1** were consistent with FABMS data, with one less methoxy singlet at δ 3.88 and one additional aromatic singlet at δ 6.33 in comparison with Ziracin. The ^{13}C NMR spectral data of **1** summarized in Table 2 confirmed the

Table 1. Physicochemical Properties and Spectral Data of Sch 58769 to Sch 58777

	Sch 58769	Sch 58771	Sch 58773	Sch 58775	Sch 58777
$[\alpha]^{20}_D$ (*c* 0.1, MeOH) (deg)	−47.2	−47.0	−45.5	−45.8	−72.3
UV max (nm)	211	211	211	213	210
	268	264	265	265	265
	305	305	305	303	305
IR max (cm^{-1})	3431, 2939, 1729	3477, 2936, 1728	3434, 2939, 1734	3430, 2937, 1734	3459, 2935, 1653
	1652, 1623, 1544	1652, 1622, 1544	1652, 1622, 1544	1653, 1623, 1543	1623, 1452, 1315
	1455, 1384, 1257	1457, 1384, 1341	1454, 1384, 1257	1457, 1385, 1345	1262, 1173, 1101
	1125, 1037	1260, 1128, 1036	1102, 1038	1258, 1172, 1036	1068, 1034, 992
molecular weight	1581	1595	1615	1645	632
FAB mass spec	1582 $(M + H)^+$	1596 $(M + H)^+$	1616 $(M + H)^+$	1646 $(M + H)^+$	633 $(M + H)^+$
molecular formula	$C_{69}H_{96}NO_{38}Cl$	$C_{70}C_{98}NO_{38}Cl$	$C_{69}H_{95}NO_{38}Cl_2$	$C_{70}H_{97}NO_{39}Cl_2$	$C_{27}H_{36}O_{17}$

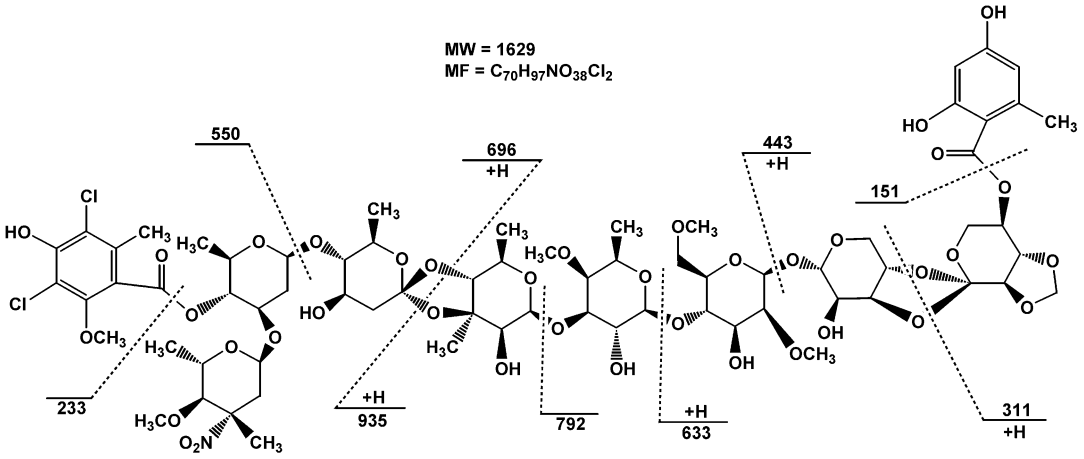

Figure 3. FABMS data of Ziracin (Sch 27899).

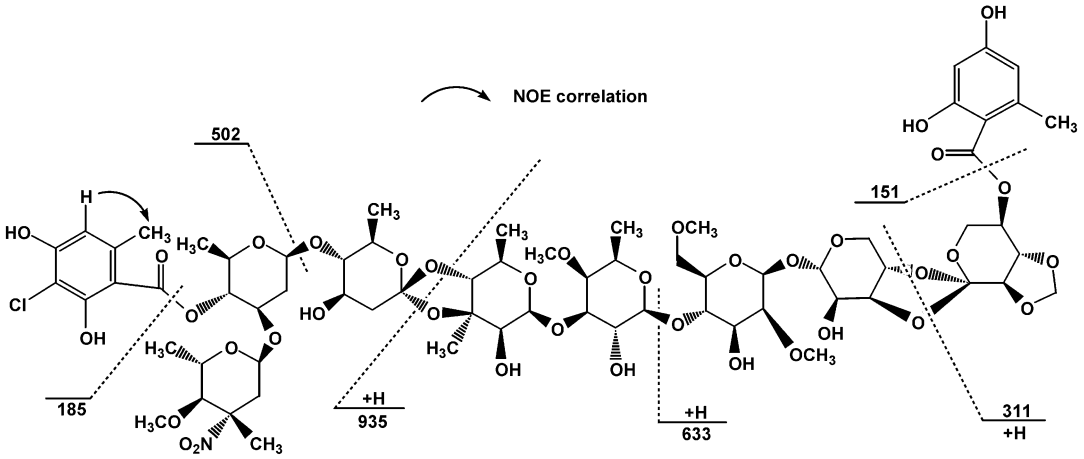

Figure 4. FABMS and NOE data of Sch 58769 (**1**).

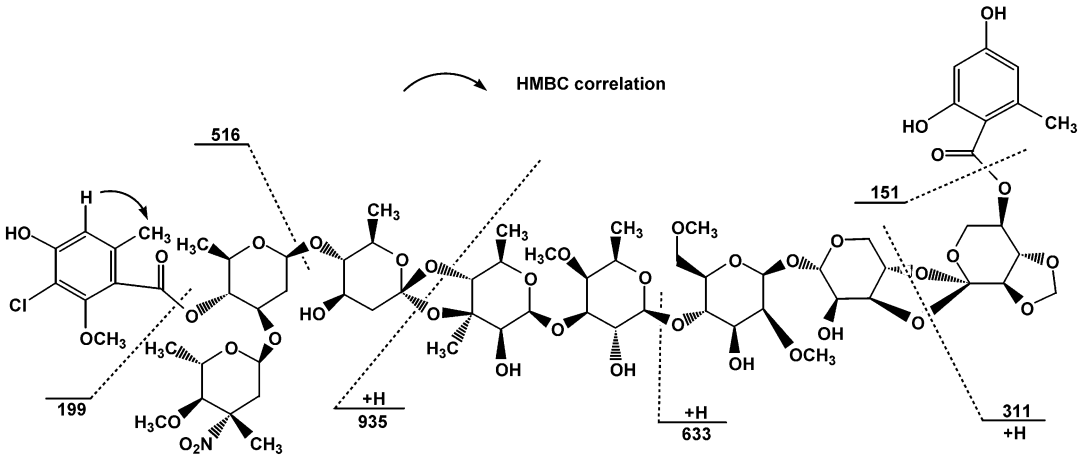

Figure 5. FABMS and HMBC data of Sch 58771 (**2**).

^{1}H NMR data by showing one less methoxy carbon in **1** compared to Ziracin. These changes suggested that one chlorine atom was substituted by hydrogen and that methoxy was replaced by a hydroxy on the left end aromatic ring in **1**. The exact position of the hydrogen was further determined by the NOE correlation of this proton to the adjacent methyl group as shown in Figure 4.

The molecular weight of **2** was found to be 1595 based on FABMS data that showed a protonated molecular ion at *m*/*z* 1596 $(M + H)^+$ and a deprotonated ion peak at *m*/*z* 1594 $(M - H)^-$ in the negative mode spectrum. The isotope cluster pattern of **2** was identical to **1**, suggesting the presence of only one chlorine atom in the molecule. Further fragmentation analysis of sequential peaks pointed out that the chlorine on the left side phenyl ring was replaced by hydrogen (34 mass units less) in comparison with Ziracin, as shown in Figure 5. The ^{1}H NMR spectral data confirmed the MS results, showing an extra aromatic proton singlet peak of δ 6.53. The position of this proton was determined by HMBC data, indicating the three-bond correlation of the methyl carbon and the proton (Figure 5).

The molecular weight of **3** was determined to be 1615 based on FABMS data that showed a protonated molecular ion peak at *m*/*z* 1616 $(M + H)^+$ and a deprotonated molecular ion at *m*/*z* 1614 $(M - H)^-$ in the negative mode spectrum. The 14 mass unit decrease of **3** suggested the

Table 2. ^{13}C NMR Data of Components **1**−**5**[a]

#	1	2	3	4	5	#	1	2	3	4	5
1	170.36 s[b]	170.58 s	170.62 s	170.44 s	170.61 s	36	75.09 d	74.66 d	75.13 d	73.76 d	
2	166.02 s	166.10 s	165.62 s	165.69 s	165.30 s	37	73.74 d	73.87 d	74.34 d	73.38 d	
3	165.21 s	165.24 s	165.28 s	165.34 s	162.62 s	38	72.77 d	72.70 d	73.90 d	72.78 d	
4	162.69 s	162.65 s	162.68 s	162.66 s	143.79 s	39	72.39 d	72.45 d	72.77 d	72.58 d	
5	156.02 s	155.86 s	152.86 s	161.55 d	119.00 s	40	71.80 t	71.85 d	72.52 d	72.08 t	
6	155.12 s	155.45 s	151.44 s	153.37 s	112.17 d	41	71.04 d	71.80 t	72.09 d	71.97 d	
7	143.78 s	143.71 s	143.76 s	151.01 s	103.65 s	42	70.99 d	71.10 d	71.92 t	71.15 d	
8	137.38 s	137.89 s	134.34 s	143.84 s	100.92 d	43	70.78 d	70.92 d	70.98 d	71.04 d	
9	120.20 s	120.12 s	120.91 s	134.57 s	97.71 d	44	70.24 d	70.71 d	70.77 d	69.95 d	
10	119.02 s	118.92 s	120.18 s	121.04 s	96.84 t	45	69.87 d	69.82 d	69.86 d	69.87 d	
11	118.33 s	118.90 s	118.99 s	120.24 s	96.47 d	46	69.83 d	69.72 d	69.79 d	68.97 d	
12	113.11 s	113.92 d	118.66 s	119.14 s	80.73 d	47	68.97 d	68.91 d	68.95 d	68.79 d	
13	112.19 d	112.61 s	113.86 s	118.09 s	80.22 d	48	68.71 d	68.59 d	68.66 d	68.77 d	
14	111.44 d	112.12 d	112.17 d	113.52 s	77.41 d	49	68.62 d	68.53 d	68.59 d	68.65 d	
15	105.16 s	104.04 d	104.09 d	112.18 d	75.17 d	50	67.96 d	67.94 d	68.00 d	68.00 d	
16	104.18 d	103.53 s	103.60 s	104.13 d	75.06 d	51	66.67 d	66.25 d	66.21 d	66.30 d	
17	104.16 d	100.97 d	100.98 d	103.48 s	73.77 d	52	63.77 t	63.64 t	63.72 t	63.33 t	
18	100.91 d	100.83 d	100.88 d	100.95 d	72.16 t	53	63.36 t	63.27 t	63.34 t	61.92 q	
19	100.53 d	100.48 d	100.45 d	100.90 d	70.76 d	54	62.01 q	61.87 q	62.18 q	61.91 q	
20	97.57 d	97.55 d	97.59 d	100.55 d	68.94 d	55	61.92 q	61.81 q	61.92 q	61.88 q	
21	96.89 t	96.79 t	96.86 t	97.47 d	68.75 d	56	60.44 q	61.56 q	61.86 q	61.11 t	
22	96.20 d	96.09d	96.14 d	95.96 d	68.45 d	57	59.03 q	60.52 q	58.96 q	60.69 q	
23	92.36 d	92.26 d	92.60 d	92.43 d	63.75 t	58	40.01 t	58.90 t	39.59 t	59.03 q	
24	90.12 s	89.94 s	90.18 s	89.90 s	63.34 t	59	38.98 t	40.16 t	35.84 t	39.91 t	
25	88.09 d	87.84 d	87.90 d	88.01 d	61.97 q	60	29.61 t	39.53 t	29.58 t	38.78 t	
26	83.93 d	84.22 d	84.21 d	84.24 d	59.11 q	61	24.44 q	35.73 t	24.36 q	35.87 t	
27	82.17 d	82.70 d	82.71 d	82.61 d	24.39 q	62	18.93 q	24.32 q	19.04 q	24.39 q	
28	80.96 d	80.91 d	80.98 d	81.37 d		63	18.77 q	18.77 q	18.62 q	19.31 q	
29	80.76 d	80.70 d	80.75 d	80.99 d		64	18.31 q	18.56 q	18.27 q	18.65 q	
30	80.36 s	80.29 s	80.34 s	80.34 s		65	18.26 q	18.22 q	18.11 q	18.32 q	
31	80.11 d	79.99 d	80.07 d	80.29 d		66	17.96 q	17.80 q	17.89 q	17.94 q	
32	79.42 d	79.36 d	79.42 d	79.40 d		67	17.89 q	17.52 q	17.57 q	17.62 q	
33	78.29 d	78.23 d	78.29 d	78.29 d		68	17.63 q	17.48 q	17.03 q	17.61 q	
34	77.41 d	77.36 d	77.23 d	77.21 d		69	15.98 q	17.47 d	16.02 q	17.48 q	
35	75.13 d	75.07 d	75.49 d	75.39 d		70		16.00 q		16.06 q	

[a] Recorded at 100 MHz in $CDCl_3$ in 10% CD_3OD treated with basic alumina. [b] Multiplicity was determined by APT/DEPT data.

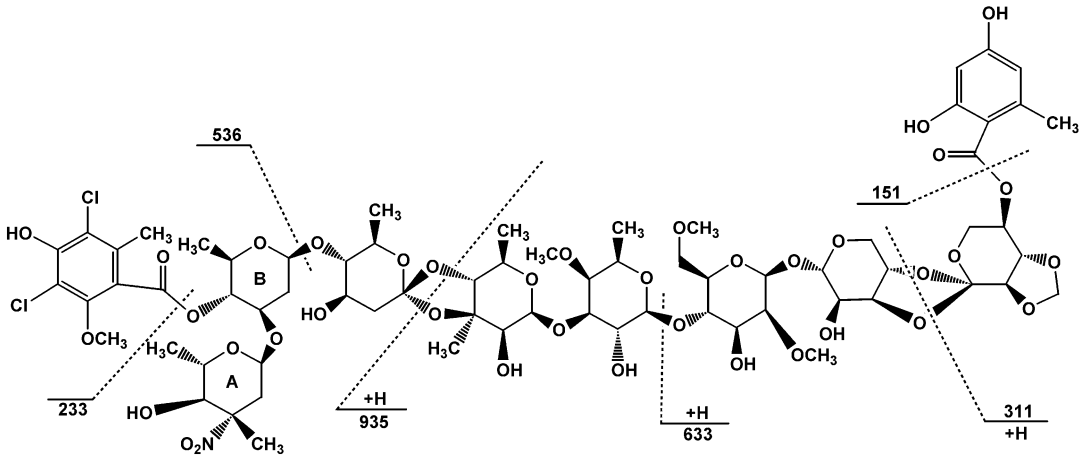

Figure 6. FABMS data of Sch 58773 (**3**).

loss of a methyl group in **3** by comparison to Ziracin. Fragmentation analysis of MS data indicated that the 14 mass unit loss occurred at the fragment of the A and B sugar residue as shown in Figure 6. Further examination of ^1H NMR data indicated one less methoxy singlet peak in the range δ 3.30−3.90 in **3** by comparison to Ziracin, suggesting that the methoxy was replaced by a hydroxy on the nitro-sugar A ring. The ^{13}C NMR data confirmed the above assignment by showing one methoxy carbon signal less than Ziracin (Table 2).

The molecular weight of **4** was found to be 1645 based on FABMS data that showed a protonated molecular ion at *m*/*z* 1646 $(M + H)^+$ and a deprotonated molecular ion at *m*/*z* 1644 $(M - H)^-$ in the negative mode spectrum. Detailed analysis of individual fragments revealed that a 16 mass unit increase in comparison with Ziracin appeared on the bicyclic ring J and K residue as shown in Figure 7. In the ^1H NMR spectrum of **4**, a formaldehyde singlet was observed at δ 8.11. Further analysis of ^1H NMR data indicated that the formaldehyde singlet replaced the dioxymethylene signal at δ 5.15 and 5.20 in comparison with Ziracin. This observation suggested the formation of a formaldehyde functionality by cleaving the methylenedioxy K ring in **4**. The assignment was confirmed by ^{13}C NMR data analysis, which indicated the presence of an aldehyde carbon at δ 161.55 and the lack of a methylenedioxy carbon at δ 97.05. As shown in Figure 7, the attachment of the formaldehyde group on the J ring was assigned on the basis of HMBC long-range coupling data that showed a three-

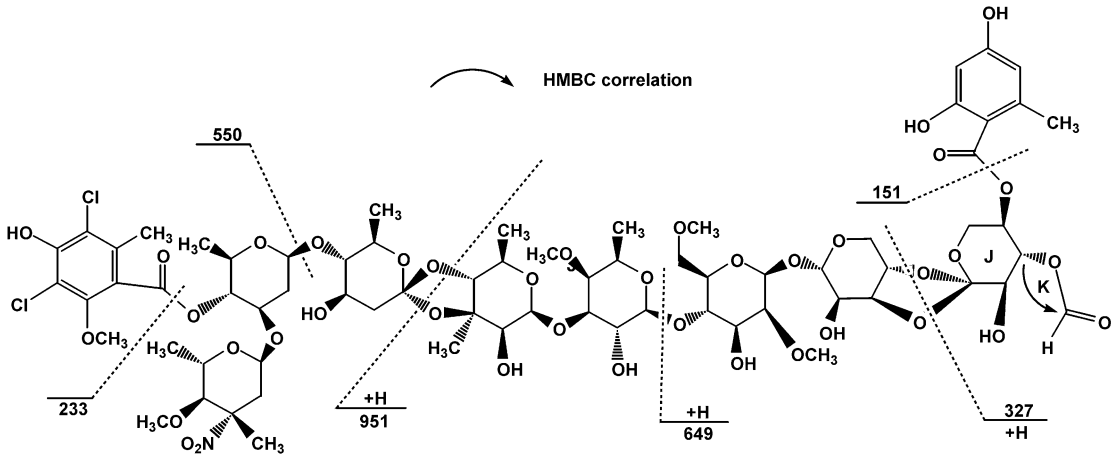

Figure 7. FABMS and HMBC data of Sch 58775 (**4**).

Table 3. Antibacterial Activity of Components **1**−**5** vs Ziracin

strain	*S. aureus* (pH 8)		*S. aureus* (pH 7)	
no.\amount:	20 μg[a]	2 μg	20 μg	2 μg
Ziracin	21[b]	19	26	23
Sch 58769 (**1**)	18	16	22	17
Sch 58771 (**2**)	17	16	20	17
Sch 58773 (**3**)	20	18	23	20
Sch 58775 (**4**)	18	15	21	17
Sch 58777 (**5**)	8	8	10	8

[a] The amount of compounds applied on each disk. [b] Zone size in mm for standard 8 mm disks.

bond correlation between the methine proton adjacent to the benzyl ester and the formaldehyde carbon.

Compound **5** was determined to be a small molecule containing only three sugar residues on the right side portion in comparison with Ziracin. In the FABMS spectrum, a protonated molecular ion at *m*/*z* 633 $(M + H)^+$ indicated the molecular weight of **5** to be 632. It was confirmed by the negative mode data that showed a deprotonated molecular ion at *m*/*z* 631 $(M - H)^-$. Unlike the previous components, the lack of isotope cluster ion in **5** suggested that there was no chlorine in the molecule. The ^{13}C NMR data were consistent with FABMS data showing only 27 carbons (Table 2). The structure of **5**, as shown in Figure 2, was proposed on the basis of extensive 2D NMR data analysis including HMQC-TOCSY and HMBC experiments.

The stereochemistry of components **1**−**5** was proposed to be the same as Ziracin based on analyses of coupling constants and NOE/NOESY spectral data in comparison with Ziracin.[10e]

The antibacterial activities of Ziracin and five analogues **1**−**5** against a *Staphylococcus aureus* strain are summarized in Table 3. The potencies of the compounds appear to be similar to Ziracin, except that component **5** showed no antibacterial activity against *S. aureus*. This evidence strongly suggests that the left side of the molecule including the nitro-sugar A ring as well as the chlorine-containing benzyl ester functionality play very important roles in the antibacterial activity of this oligosaccharide family of compounds.

Experimental Section

General Experimental Procedures. Optical rotations were measured on a Perkin-Elmer 243B polarimeter. IR and UV spectra were obtained using a Nicolet FTIR model 10-MX and Hewlett-Packard "8050 A" UV−vis spectrophotometer, respectively. FABMS data were produced by a VG ZAB-SE mass spectrometer in a glycerol-thioglycerol matrix. Both ^1H and ^{13}C NMR spectra were recorded using Varian XL-400 instruments operating at 400 and 100 MHz, respectively.

Fermentation. The frozen culture (1 mL) of *Micromonospora carbonacea* subspecies Africana, strain PF6-3, was transferred into a 300 mL Erlenmeyer shake flask containing 100 mL of seed medium. The medium composition was as follows (g/L): beef extract (Difco) 3, Tryptone (Difco) 5, Cerelose (CPC; 2001) 1, potato dextrin (Avebe, WPD-650) 24, yeast extract (Universal, Tastone) 5, calcium *carbonae* (Pfizer, Albaglos) 1, and silicone defoamer (Union Carbide, SAG-471, 30% suspension) 0.3 mL/L. The flask was incubated 48 h at 30 °C with agitation (300 rpm, 1 in. stroke), and 30 mL of the culture was transferred to 6 × 2 L flasks, each containing 500 mL of the same seed medium. Following 48 h of incubation as before, the 3 L culture was transferred into an inoculation fermenter containing 300 L of the same medium for an additional 24 h of cultivation. Finally, the contents of the inoculation fermenter were transferred to a larger fermenter containing 10 000 L of production medium. The composition of the production medium was as follows (g/L): yeast extract 5, meat peptone (Marcor, type PS) 6, Cerelose 22, corn steep powder (Marcor) 2, potato dextrin 60, boiled linseed oil (Kleenstreep) 4, calcium carbonate 4, cobalt chloride 5 H_2O (Mallinckrodt) 0.002, and silicone defoamer 0.5 mL/L. The fermentation was conducted at 36 °C for 130 h under aeration and agitation maintaining the dissolved oxygen between 50 and 100% saturation. The fermentation was carried out with 80−240 standard cubic feet per minute air flow for about 125 h.

Initial Isolation. The fermentation broth (5000 L) was mixed with XAD-7 resin (300 L, Rohm & Haas) under the basic conditions at pH 10.5 to adsorb the active components. The resin beads were separated from the broth and small mycelial particles by sieving. Tap water was used to wash the resin free from broth and mycelia. The adsorbed resin was then charged to a tapered column (500 L). The column was washed with additional deionized water (1000 L) and then eluted with EtOAc (900 L). The antibiotic complex containing cuts were combined and concentrated under vacuum. The concentrate (∼45 L) was precipitated with heptane (100 L). The precipitate was filtered and dried in a vacuum at 25 °C to obtain ∼5 kg of crude material. To oxidize the nitroso component in the antibiotic complex, a catalytical oxidation reaction was performed using *tert*-butyl hydroperoxide (5.5 L, 3 M solution in 2,2,4-trimethylpentane)/sodium bicarbonate (2 kg) in the presence of vanadyl acetylacetonate (50 g) as a catalyst.

The crude oxidized complex (2.5 kg) was applied on a bare irregular silica gel column (70−25 μm) in isopropyl acetate. The column was eluted with isopropyl acetate. Functions 1, 2, and 3 were collected as 200 L cuts. The antibiotic components were monitored by analytical HPLC. The head cut fractions 3 and 4, which were enriched in minor components, were combined and vacuum concentrated to about 6 L at lower

than 30 °C. The concentrated solution was precipitated by adding 12 L of heptane with agitation. The precipitate was filtered and dried in a vacuum oven at 25 °C to obtain 0.4 kg of powdery material. The tail cut fractions 12−15, which were enriched in other minor components, were combined and processed in a similar manner to obtain 0.2 kg of product.

Analytical HPLC for monitoring the fractionated samples was under the following isocratic conditions: PVA-Sil, 5 μm, 150 × 4.6 mm, CH_2Cl_2/MeOH (98:2), 2 mL/min, 20 min, UV = 265 nm.

Antibacterial Assay. All components were tested for activity based on an agar disk-diffusion protocol. Each component was dissolved at 1 mg/mL in CH_2Cl_2/MeOH (95:5 v/v) and a 10-fold dilution made in the same vehicle. Twenty microliters of each concentration was transferred to an 8 mm standard paper disk and allowed to air-dry for 30 min. Each set of disks was placed on agar seeded with *S. aureus* at two pH's (7 and 8) and incubated overnight at 35 °C. Zone sizes of inhibition are given as the diameter of the circle of inhibition in millimeters.

Sch 58769 (1): ^{1}H NMR ($CDCl_3$−CD_3OD, 400 MHz) δ 6.36 (1H, s), 6.20 (2H, br.s), 5.37 (1H, dt, J = 5, 9 Hz), 5.19 (1H, d, J = 1.5 Hz), 5.11, 5.17 (2H, s, OCH_2O), 5.06 (1H, t, J = 9, 9 Hz) 4.97 (1H, s), 4.93 (1H, d, J = 1 Hz), 4.71 (1H, s), 4.52 (1H, dd, J = 4.5, 10 Hz), 4.40 (1H, br s), 4.38 (1H, m), 4.21 (1H, m), 4.18 (1H, d, J = 5 Hz), 4.11 (1H, m), 4.02 (1H, br s), 3.98 (1H, t, J = 9.5 Hz), 3.73−3.95 (10H, m), 3.72 (1H, dd, J = 9, 11.5 Hz), 3.52−3.66 (5H, m), 3.55 (3H, s), 3.53 (3H, s), 3.42 (2H, m), 3.33 (3H, s), 3.31 (1H, br s), 3.26 (1H, m) 3.20 (3H, s), 3.02 (1H, t, J = 9 Hz), 2.42 (3H, s), 2.39 (3H, s), 2.35 (1H, dd, J = 5, 13.5 Hz), 2.32 (1H, m), 2.00 (1H, dd, J = 2, 13.5 Hz), 1.76 (1H, t, J = 12.5 Hz), 1.65 (1H, dt, J = 10, 12 Hz), 1.62 (1H, m), 1.49 (2H, s), 1.38 (1H, m), 1.29 (3H, s), 1.26 (3H, d, J = 6 Hz), 1.20 (3H, s), 1.18 (3H, d, J = 6 Hz), 1.09 (1H, m). 0.97 (3H, d, J = 6 Hz), 0.84 (3H, d, J = 6 Hz); *anal.* C 52.21%, H 6.18%, N 0.78%, Cl 2.01%, calcd for $C_{69}H_{96}NO_{38}Cl$, C 52.37%, H 6.09%, N 0.89%, Cl 2.21%.

Sch 58771 (2): ^{1}H NMR ($CDCl_3$−CD_3OD, 400 MHz) δ 6.56 (1H, s), 6.19 (2H, br s) 5.36 (1H, dt, J = 5, 9 Hz), 5.18 (1H, d, J = 1.5 Hz), 5.10, 5.16 (2H, s, OCH_2O), 4.97 (1H, d, J = 1 Hz), 4.93 (1H, m), 4.91 (1H, t, J = 9 Hz), 4.71 (1H, s), 4.50 (1H, dd, J = 1.5, 10 Hz), 4.40 (1H, br s), 4.37 (1H, dt, J = 4.5, 10 Hz), 4.21 (1H, dd, J = 9, 11 Hz), 4.16 (1H, d, J = 7.5 Hz), 4.11 (1H, dd, J = 4.5, 9 Hz), 4.02 (1H, d, J = 1.5 Hz), 3.97 (1H, t, J = 9 Hz), 3.73−3.95 (10H, m), 3.83 (3H, s), 3.71 (1H, dd, J = 9, 11.5 Hz), 3.52−3.66 (8H, m), 3.56 (3H, s), 3.54 (3H, s), 3.47 (1H, m), 3.42, (2H, m), 3.33 (3H, s), 3.28 (3H, s), 3.03 (1H, t, J = 9 Hz), 2.42 (3H, s), 2.38 (1H, dd, J = 5, 12.5 Hz), 2.31 (1H, m), 2.29 (1H, m), 2.26 (3H, s), 2.01 (1H, dd, J = 2, 13.5 Hz), 1.76 (1H, t, J = 12.5 Hz), 1.68 (1H, dt, J = 10, 12.5 Hz), 1.61 (3H, s), 1.37 (3H, d, J = 6 Hz), 1.29 (3H, s), 1.28 (3H, d, J = 6 Hz), 1.21 (3H, d, J = 6 Hz), 1.20 (3H, d, J = 6 Hz), 0.86 (3H, d, J = 6 Hz); *anal.* C 53.38%, H 6.76%, N 0.81%, Cl 2.25%, calcd for $C_{70}H_{98}NO_{38}Cl$, C 52.66%, H 6.14%, N 0.88%, Cl 2.19%.

Sch 58773 (3): ^{1}H NMR ($CDCl_3$−CD_3OD, 400 MHz) δ 6.18 (2H, br s), 5.34 (1H, dt, J = 5, 9 Hz), 5.16 (1H, d, J = 1.5 Hz), 5.09, 5.14 (2H, s, OCH_2O), 4.96 (1H, br s), 4.90 (1H, t, J = 9 Hz), 4.69 (1H, s), 4.49 (1H, dd, J = 1.5, 10 Hz), 4.38 (1H, br.s), 4.34 (1H, dt, J = 4.5, 10 Hz), 4.19 (1H, dd, J = 9, 11 Hz), 4.15 (1H, d, J = 7.5 Hz), 4.10 (1H, dd, J = 4.5, 9 Hz), 4.02 (1H, d, J = 1.5 Hz), 3.98 (1H, t, J = 9 Hz), 3.73−3.93 (10H, m), 3.83 (3H, s), 3.70 (1H, dd, J = 9, 11.5 Hz), 3.50−3.65 (4H, m), 3.55 (3H, s), 3.53 (3H, s), 3.41 (2H, m), 3.40 (1H, m), 3.32 (3H, s), 3.02 (1H, t, J = 9 Hz), 2.41 (3H, s), 2.38 (1H, dd, J = 4.5, 12.5 Hz), 2.33 (3H, s), 2.31 (1H, m), 2.28 (1H, m), 2.11 (1H, dd, J = 1.5, 13.5 Hz), 1.75 (1H, t, J = 12.5 Hz), 1.69 (1H, dt, J = 10, 12.5 Hz), 1.66 (3H, s), 1.37 (3H, d, J = 6 Hz), 1.28 (3H, s), 1.26 (3H, d, J = 6 Hz), 1.20 (3H, d, J = 6 Hz), 1.19 (3H, d, J = 6 Hz), 0.81 (3H, d, J = 6 Hz); *anal.* C 51.89%, H 5.96%, N 0.81%, Cl 4.12%, calcd For $C_{69}H_{95}NO_{38}Cl_2$, C 51.27%, H 5.88%, N 0.87%, Cl 4.33%.

Sch 58775 (4): ^{1}H NMR ($CDCl_3$−CD_3OD, 400 MHz) δ 8.22 (1H, s, CHO), 6.20 (1H, d, J = 2 Hz), 6.19 (1H, d, J = 2 Hz), 5.47 (1H, t, J = 9 Hz), 5.25 (1H, dt, J = 5, 9 Hz), 5.18 (1H, d, J = 1 Hz), 4.99 (1H, d, J = 1 Hz), 4.94 (1H, dd, J = 2, 5 Hz), 4.90 (1H, t, J = 9 Hz), 4.71 (1H, s), 4.51 (1H, dd, J = 1, 10 Hz), 4.41 (1H, br s), 4.35 (1H, dt, J = 4.5, 10 Hz), 4.18 (1H, d, J = 7.5 Hz), 4.11 (1H, dd, J = 4.5, 9 Hz), 4.03 (1H, br s), 3.96 (1H, dd, J = 9, 11 Hz), 3.73−3.93 (10H, m), 3.84 (3H, s), 3.52−3.66 (5H, m), 3.56 (3H, s) 3.55 (3H, s), 3.45 (1H, m), 3.41 (2H, m), 3.34 (3H, s), 3.31 (3H, s), 3.03 (1H, t, J = 9 Hz), 2.37 (3H, s), 2.34 (3H, s), 2.30 (1H, dd, J = 4.5, 12.5 Hz), 2.01 (1H, dd, J = 2, 13.5 Hz), 1.78 (1H, t, J = 12.5 Hz), 1.71 (1H, dt, J = 10, 12.5 Hz), 1.63 (3H, s), 1.39 (3H, d, J = 6 Hz), 1.31 (3H, s), 1.29 (3H, d, J = 6 Hz), 1.28 (3H, d, J = 6 Hz), 1.21 (3H, d, J = 6 Hz), 0.83 (3H, d, J = 6 Hz); *anal.* C 51.35%, H 6.01%, N 0.81%, Cl 4.11%, calcd for $C_{70}H_{97}NO_{39}Cl_2$, C 51.06%, H 5.90%, N 0.85%, Cl 4.26%.

Sch 58777 (5): ^{1}H NMR ($CDCl_3$−CD_3OD, 400 MHz) δ 6.20 (1H, d, J = 2 Hz), 6.18 (1H, d, J = 2 Hz), 5.35 (1H, dt, J = 5, 9 Hz), 5.19 (1H, d, J = 1.5 Hz), 5.09, 5.14 (2H, s, OCH_2O), 4.72 (1H, s), 4.40 (1H, br s) 4.38 (1H, dt, J = 4.5, 10 Hz), 4.20 (1H, dd, J = 9, 11 Hz), 4.11 (1H, dd, J = 4.5, 9 Hz), 3.99 (1H, t, J = 10 Hz), 3.91 (1H, dd, J = 4.5, 10 Hz), 3.78 (1H, t, J = 10 Hz), 3.71 (1H, dd, J = 4.5, 11 Hz), 3.60, 3.68 (2H, d, J = 9 Hz, CH_2O), 3.57 (1H, m), 3.56 (3H, s), 3.41−3.51 (3H, m), 3.34 (3H, s), 3.28 (1H, m), 2.41 (3H, s); *anal.* C 51.11%, H 5.58%, calcd for $C_{27}H_{36}O_{17}$, C 51.27%, H 5.70%.

Acknowledgment. The authors are grateful to Mr. S. Mittleman for IR data, and Mr. G. Torraca for optical rotation and elemental analysis data. We also thank Ms. D. Scott for the preparation of the manuscript.

References and Notes

(1) Richet, H.; Mohammed, J.; McDonald, L. C.; Jarvis, W. R. *Emerging Infect. Dis.* **2001**, *7*, 319−322.
(2) Richet, H. M. *Am. Soc. Microbiol News* **2001**, *67*, 304−309.
(3) Courvalin, P.; Trieu-Cuot, P. *Clin. Infect. Dis.* **2001**, *33* (Suppl. 3), S138−146.
(4) Sieradzki, K.; Tomasz, A. *FEMS Microbiol. Lett.* **1996**, *142*, 161−166.
(5) Jones, R. N.; Barrett, M. S. *Clin Microbiol. Infect.* **1995**, *1*, 35−43.
(6) Hare, R. S.; Sabatelli, F. J. *Abstr. 38th Intersci, Conf. Antimicrob. Agents Chemother.* **1998**, *Abstr. E-119*, p 204.
(7) (a) McNicholas, P. M.; Mann, P. A.; Najarian, D. J.; Miesel, L.; Hare, R. S.; Black, T. A. *Antimicrob. Agents Chemother.* **2001**, *45*, 79−83. (b) Adrian, P. V.; Mendrick, C.; Loebenberg, D.; McNicholas, P.; Shaw, K. J.; Klugman, K. P.; Hare, R. S.; Black. T. A. *Antimicrob. Agents Chemother.* **2000**, *44*, 3101−3106. (c) Aarestrup, F. M.; Jensen, L. B. *Antimicrob. Agents Chemother.* **2000**, *44*, 3425−3427. (d) McNicholas, P. M.; Najarian, D. J.; Mann, P. A.; Hesk, D.; Hare, R. S.; Shaw, K. J.; Black, T. A. *Antimicrob. Agents Chemother.* **2000**, *44*, 1121−1126. (e) Adrian, P. V.; Zhao, W.; Black, T. A.; Shaw, K. J.; Hare, R. S.; Klugman, K. P. *Antimicrob. Agents Chemother.* **2000**, *44*, 732−738.
(8) Chu, M.; Mierzwa, R.; Patel, M.; Jenkins, J.; Das, P.; Pramanik, B.; Chan, T.-M. *Tetrahedron Lett.* **2000**. *41*, 6689−6693.
(9) (a) Horan, A.; Brodsky, B. *Int. J. Syst. Bacterial.* **1964**, *32*, 195−200. (b) Waitz, J. A.; Patel, M. G.; Marquez, J. A.; Kalyanpur, M. G.; Horan, A. C. U.S. Patent 4,597,968, 1986.
(10) (a) Ganguly, A. K.; Pramanik, B.; Chan, T.-M.; Sarre, O.; Liu, Y.-T.; Morton, J.; Girijavallabhan, V. *Heterocycles* **1989**, *28*, 83−88. (b) Ganguly, A. K.; Sarre, O. Z.; McPhail, A. T.; Miller, R. *J. Chem. Soc., Chem. Commun.* **1979**, *35*, 529−532. (c) Ganguly, A. K.; Sarre, O. Z.; Greeves, D.; Morton, J. *J. Am. Chem. Soc.* **1975**, *97*, 1982−1985. (d) Chan, T.-M.; Osterman, R. M.; Morton, J.; Ganguly, A. K. *Magn. Reson. Chem.* **1997**, *35*, 529−532. (e) Ganguly, A. K.; McCormick, J. L.; Chan, T.-M.; Saksena, A. K.; Das, P. R. *Tetrahedron Lett.* **1997**, 7989−7992.

NP020093T